

# Psychosocial Stress and Cannabinoid Drugs Affect Acetylation of $\alpha$ -tubulin (K40) and Gene Expression in the Prefrontal Cortex of Adult Mice

Jordi Tomas-Roig (✉ [jordi.tomas-roig@med.uni-goettingen.de](mailto:jordi.tomas-roig@med.uni-goettingen.de))

University Medical Center Göttingen

**Shyam Sundar Ramasamy**

University Medical Center Göttingen

**Diana Zbarsky**

University Medical Center Göttingen

**Ursula Havemann-Reinecke**

University Medical Center Göttingen

**Sigrid Hoyer-Fender**

Johann-Friedrich-Blumenbach-Institute of Zoology and Anthropology – Developmental Biology, GZMB, Georg-August-University Göttingen

---

## Research Article

**Keywords:** Psychosocial stress, cannabinoid drugs,  $\alpha$ -tubulin (K40), gene expression, prefrontal cortex, adult mice

**Posted Date:** December 7th, 2021

**DOI:** <https://doi.org/10.21203/rs.3.rs-1119831/v1>

**License:**  This work is licensed under a Creative Commons Attribution 4.0 International License.

[Read Full License](#)

---

# Abstract

The dynamics of neuronal microtubules are essential for brain plasticity. Vesicular transport and synaptic transmission, additionally, requires acetylation of  $\alpha$ -tubulin, and aberrant tubulin acetylation and neurobiological deficits are associated. Prolonged exposure to a stressor or consumption of drugs of abuse, like marijuana, lead to neurological changes and psychotic disorders. Here, we studied the effect of psychosocial stress and the administration of cannabinoid receptor type 1 drugs on  $\alpha$ -tubulin acetylation in different brain regions of mice. We found significantly decreased tubulin acetylation in the prefrontal cortex and the dorsal striatum in stressed mice. The impact of cannabinoid drugs on stress-induced microtubule disturbance was investigated by administration of the cannabinoid receptor agonist WIN55,212-2 and/or antagonist rimonabant. In both, control and stressed mice, the administration of WIN55,212-2 significantly increased the tubulin acetylation in the prefrontal cortex whereas administration of both cannabinoid drugs acted antagonistically indicating a cannabinoid receptor type 1 mediated effect. The analysis of gene expression in the prefrontal cortex showed a consistent expression of *ApoE* attributable to either psychosocial stress or administration of the cannabinoid agonist. Additionally, *ApoE* expression inversely correlated with acetylated tubulin levels when comparing controls and stressed mice treated with WIN55,212-2 whereas rimonabant treatment showed the opposite.

## Introduction

Environmental factors such as traumatic events and consumption of drugs of abuse like cannabinoids can induce psychotic disorders as a result of neurobiological changes. These alterations comprise dysfunctions in neurogenesis, axonal growth, myelination, synaptogenesis, synaptic pruning, and neuroendocrine regulation<sup>1</sup>. For instance, preclinical studies indicated that chronic exposure to psychosocial stress can cause neuroanatomical changes as e.g. inhibition of adult neurogenesis in the dentate gyrus, or dendritic atrophy in the hippocampus (HIPPO) and the prefrontal cortex (PFC)<sup>2-5</sup>. Furthermore, chronic exposure to stress compromised the stability and function of axonal microtubules (MTs) promoting the hyperphosphorylation of the microtubule-binding protein Tau, and the formation of neurofibrillary tangles<sup>6,7</sup>. Cytoskeletal alterations have also been reported in several neuropsychiatric diseases such as schizophrenia, major depressive disorder, and bipolar disorder. A common hallmark underlying neuropsychiatric disorders comprises an aberrant expression of tubulin isoforms and tubulin acetylation<sup>8,9</sup>.

MTs are assembled from stable heterodimers of  $\alpha/\beta$ -tubulin and are constantly remodeled. In neuronal cells, MTs are important for compartmentation, rigidity, long-distance transport, and synaptic transmission<sup>10</sup>. Although they are highly conserved in evolution, MTs adapt to diverse cellular functions through microtubule-associated proteins (MAPs), posttranslational modifications of tubulins (PTMs), and binding proteins for specific PTMs. Thus, posttranslational modifications generate a 'tubulin code' that specifies the assignment and coordination of the complex functions of MTs<sup>11-13</sup>. An important modification is the acetylation of  $\alpha$ -tubulin at lysine 40 ( $\alpha$ -tubulin K40ac) that has been generally

associated with MT stability. The addition of acetyl groups does not alter the MT ultrastructure but it is required for vesicular transport<sup>14,15</sup>. The major tubulin acetyltransferase in mammals is the  $\alpha$ -tubulin acetyltransferase 1 (ATAT1) causing complete loss of tubulin acetylation when deleted in mice. Although the loss of ATAT1 is not life-threatening, rodents underwent an enlargement of the forebrain lateral ventricles pointing out an important biological function of the *Atat1*-gene in this brain area<sup>16–18</sup>. Deacetylation of  $\alpha$ -tubulin at K40ac is achieved by the histone deacetylase 6 (HDAC6) and the sirtuin type 2 (SIRT2), which, additionally, deacetylate further substrates<sup>19,20</sup>. In the rodent brain, the main  $\alpha$ -tubulin deacetylase is HDAC6<sup>21</sup>. Additionally, HDAC6 recruits polyubiquitinated proteins to aggresomes and controls the fusion of autophagosomes and lysosomes<sup>22–24</sup>. HDAC6 is, therefore, involved in the clearance of misfolded proteins and protein aggregates<sup>25,26</sup>. Furthermore, HDAC6 activity has been associated with emotional behavior like activity, anxiety, and depression<sup>27,28</sup>. Thus, MTs in general and HDAC6, in particular, came into focus as promising therapeutic targets for neuropsychiatric disorders<sup>29,30</sup>. To this end, HDAC inhibitors are emerging as potential antidepressant drugs<sup>31</sup>.

Under physiological conditions, synaptic transmission and tissue homeostasis are biological mechanisms regulated by the cannabinoid receptor type-1 through G protein-coupled receptors (GPCRs)<sup>32</sup>. The cannabinoid receptor type-1 (CB1) is highly expressed in the brain and, specifically, found in axons and presynaptic terminals<sup>33</sup>. Upon stress exposure, CB1 and its endogenous ligands compromise the proper function of the brain<sup>34</sup>. CB1 mediates the pharmacological actions of synthetic cannabinoid drugs such as the full cannabinoid agonist WIN55,212-2 (referred to as W) and the inverse agonist rimonabant (referred to as R)<sup>35</sup>. Activation of CB1 by endogenous or exogenous cannabinoids regulates neuronal metabolism by decreasing mitochondrial cAMP and PKA<sup>36</sup>. Under pathological conditions of prolonged exposure to a stressor, the expression of CB1 is compromised<sup>32,35</sup>. Socially defeat mice display a variety of molecular and physiological changes, commonly reported in psychiatric disorders, including changes in the endocannabinoid system and deregulation of  $\beta$ -actin contributing to dendritic and synaptic dysfunctions<sup>7,37,38</sup>.

Here, we used a long-term psychosocial defeat protocol as a stress model for its etiological, predictive, discriminative, and face validity<sup>39</sup>. In our model, mice were exposed to daily psychosocial stress and finally acutely treated with the full cannabinoid agonist W and/or the inverse agonist R. We hypothesized that MTs might be affected in stressed animals, and thus, treatment with cannabinoid drugs could confer neuroprotection by remodeling the MT system. For this purpose, we evaluated stressed animals treated with cannabinoid drugs by quantifying  $\alpha$ -tubulin acetylation and assessing differential gene expression. Among the wide spectrum of cerebral regions closely involved in stress-related disorders (for review see Ref.<sup>40</sup>), we directed our investigation on the PFC, a brain structure critically involved in social behaviour<sup>41,42</sup>.

## Results

# Psychosocial stress affects tubulin acetylation in the brain

We first asked whether the cytoskeleton was affected by repeated psychosocial stress. To this end, we investigated  $\alpha$ -tubulin acetylation at K40 in different brain regions of stressed (STS) mice and control (CTR) mice by quantitative immune-blotting. In each experimental setting four biological replicates, i.e., four individual male mice were investigated, and every probe was loaded several times. The protein lysates of all biological replicates were treated and analysed simultaneously. Acetylated  $\alpha$ -tubulin (K40) and  $\beta$ -actin were indirectly detected by fluorophore-labelled secondary antibodies, and the relative quantities of acetylated  $\alpha$ -tubulin and their fold-change differences were calculated in the manner described previously. Fold changes of all technical and biological replicates were combined in Fig. 1 (CTR vs STS, all brain regions). We observed a decrease of  $\alpha$ -tubulin acetylation in stressed animals compared to the control animals in the PFC, the HIPP, and the dorsal striatum (DS), whereas an opposite pattern was observed in the cerebellum (CRB). The changes in  $\alpha$ -tubulin acetylation were statistically significant for the PFC ( $t(34)=3.903$ ;  $p<0.001^{***}$ ) and the DS ( $t(35)=2.702$ ;  $p=0.0106^*$ ). No significant differences were found for HIPP ( $t(37)=1.696$ ;  $p=0.0984$ ) and CRB ( $t(29)=1.662$ ;  $p=0.1075$ ). Subsequently, our data indicate that psychosocial stress affects the acetylation of  $\alpha$ -tubulin in the PFC and the DS. Since the PFC is critically involved in social behavior<sup>41,42</sup>, we aimed to further characterize this brain structure by assessing which genes were differentially expressed when comparing stressed and control mice subjected to different pharmacological interventions.

## Administration of the cannabinoid receptor agonist promotes tubulin acetylation in the prefrontal cortex

Since our results demonstrated an effect of psychosocial stress on acetylation of tubulin in the brain, having a presumable detrimental outcome on the cytoskeletal organization, stability, and function, we wondered whether cannabinoid treatments might be effective in overcoming the stress-induced impact on MTs and neural function. We focused here on the PFC due to its particular importance for social behaviour and intellectual abilities, along with the highly significant decrease of tubulin acetylation in stressed animals (Fig. 1). The two way ANOVA revealed a significant effect of stress ( $F(1, 29)= 29.35$ ;  $p<0.001^{***}$ ), drug treatment ( $F(3, 29)= 7.56$ ;  $p=0.001^{***}$ ) as well as a significant interaction (stress x drug) ( $F(3, 29)= 3.91$ ;  $p=0.022^*$ ). The interaction of stress and drug treatment was evaluated by multiple comparisons post hoc tests (Table 1). Bonferroni post hoc test revealed higher expression of acetylated tubulin in controls treated with either vehicle or the CB1 agonist when compared to their stressed counterparts ( $p=0.0091^{**}$ ;  $p=0.021^*$ , respectively) (Table 1; Fig. 2). The use of cannabinoid receptor agonist in controls increased the expression of acetylated tubulin in contrast to the control group treated with the antagonist ( $p=0.014^*$ ) (Table 1; Fig. 2) and also did so when both drugs were administered simultaneously under stress conditions in comparison with those subjected to stress and treated with the cannabinoid antagonist ( $p=0.033^*$ ) (Table 1; Fig. 2). Thus, our results indicate that treatment with the CB1 agonist protects from stress-induced tubulin deacetylation while the administration of the antagonist favours the removal of acetyl groups in the PFC.

Table 1

Acetylated  $\alpha$ -tubulin profile in the prefrontal cortex of control and stressed mice upon vehicle or cannabinoid drug exposure. Column titles from left to right: Levene's test; One-way ANOVA; Pairwise comparisons;  $(M_i - M_j) + SD$ ; p-value. CTR, control; STS, stress; V, vehicle; W, WIN55,212-2; R, rimonabant;  $(M_i - M_j) + SD$ , average difference between 2 distinct treatments including the standard deviation.

	Equality of variances (Levene test)		One-way ANOVA					
						Pairwise comparisons	$(M_i - M_j) + SD$	p value
Acetylated tubulin	W(7,22)=0.99	n.s.	F(7,22)=8.84	***	<0.001	CTR V+V vs STS V+V	0.41+0.01	.009
Expression						CTR V+W vs STS V+W	0.43+0.11	.021
						CTR V+W vs CTR R+V	0.42+0.10	.014
						CTR V+W vs STS R+V	-0.35+0.09	.033
						STS R+V vs STS R+W		

## Acetylation of $\alpha$ -tubulin in the hippocampus, the dorsal striatum, and the cerebellum after administration of cannabinoid drugs

We also investigated  $\alpha$ -tubulin acetylation in the HIPP, the DS, and the CRB after administration of either the cannabinoid receptor 1 agonist W, the inverse agonist R, or both cannabinoid drugs in both stressed and control animals. In the HIPP of control animals, administration of R+V caused a decrease in tubulin acetylation ( $t(26)=3.577$ ;  $p=0.0014^{***}$ ) whereas neither V+W nor R+W resulted in a significant change in comparison to the control group treated with vehicle alone (Fig. 3, panel A). In stressed animals, which showed already a significant reduction in tubulin acetylation ( $t(30)=2.234$ ;  $p=0.0331^*$ ) when compared to controls subjected to V+V, the administration of either V+W or both R+W led to a remarkable reduction of tubulin acetylation as compared to the vehicle-treated animals subjected to long term stress (V+W:  $t(32)=2.364$ ;  $p=0.0243^*$ ; R+W:  $t(36)=2.367$ ;  $p=0.0235^*$ ), whereas administration of the antagonist did not significantly change tubulin acetylation levels (Fig. 3, panel A).

In the DS of control mice, the administration of either V+W, R+W, or both R+W did not alter tubulin acetylation status whereas in stressed animals a significant reduction of tubulin acetylation was determined in controls (STS, V+V vs CTR, V+V,  $t(26)=2.660$ ;  $p=0.0132^*$ ) and remarkably, when R+V was administered ( $t(27)=2.631$ ;  $p=0.0139^*$ ) (Fig. 3, panel B).

In the CRB of control animals, the administration of either V+W, R+W, or R+V induced a significant decrease in tubulin acetylation as compared to the vehicle-treated controls (CTR, V+V vs V+W :  $t(24)=3.102$ ;  $p=0.0049^{**}$ ; V+V vs R+W:  $t(23)=2.896$ ;  $p=0.0082^{**}$ ; V+V vs R+V:  $t(23)=3.793$ ;  $p=0.0009^{***}$ ) (Fig. 3, panel C). Stressed animals treated with vehicle did not display significantly different tubulin acetylation than their matched controls. Furthermore, the administration of either V+W, R+V, or both cannabinoid drugs did not change tubulin acetylation in stressed animals compared to socially-defeat animals subjected to vehicle alone (Fig. 3, panel C).

To conclude, the effect on tubulin acetylation by either long-term exposure to stress or administration of cannabinoid drugs was different according to the brain region but especially prominent in the PFC. The effects of stress are brain-region-specific as pointed out previously<sup>43</sup>.

## Gene expression signature in the prefrontal cortex

We reported changes in gene expression in the PFC when socially defeat mice were subjected to cannabinoid drugs by use of the digital transcript counting (nCounter) assay (NanoString)<sup>35</sup>. Long term exposure to psychosocial stress increased the expression of *ApoE* ( $t(6)=6.61$ ;  $p_{adj}=0.01^{**}$ ), *Cxcl12* ( $t(6)=6.47$ ;  $p_{adj}=0.02^*$ ), *Dtnbp1* ( $t(6)=5.85$ ;  $p_{adj}=0.02^*$ ), *Ski* ( $t(6)=5.16$ ;  $p_{adj}=0.04^*$ ), and *Cnr1* ( $t(6)=4.71$ ;  $p_{adj}=0.05^*$ ) when compared to their matched controls (Table 2). Non-stressed animals treated simultaneously with both drugs underwent a remarkable downregulation of *ApoE* ( $t(6)=-7.92$ ;  $p_{adj}<0.001^{***}$ ) and *Rtn4r* ( $t(6)=-9.12$ ;  $p_{adj}<0.001^{***}$ ) in comparison with their controls (Table 2). The administration of R+W in non-stressed mice resulted in lower levels of *ApoE* ( $t(6)=11.07$ ;  $p_{adj}<0.001^{***}$ ), *Rtn4r* ( $t(6)=11.77$ ;  $p_{adj}<0.001^{***}$ ), *Vgf* ( $t(6)=7.4$ ;  $p_{adj}=0.01^{**}$ ), *Rxra* ( $t(6)=6.92$ ;  $p_{adj}=0.01^{**}$ ), *Cnp* ( $t(6)=5.6$ ;  $p_{adj}=0.02^*$ ), *Mbp* ( $t(6)=4.72$ ;  $p_{adj}=0.05^*$ ), and *Cnr1* ( $t(6)=6.64$ ;  $p_{adj}=0.03^*$ ) than the control group treated with V+W (Table 2). Daily exposure to psychosocial stress induced a decrease in *Mag* expression upon V+W administration ( $t(6)=5.73$ ;  $p_{adj}=0.04^*$ ) in contrast to those exposed to vehicle alone (Table 2). Social defeat mice treated with R+V displayed lower expression of *ApoE* ( $t(6)=-8.96$ ;  $p_{adj}=0.02^*$ ) than those treated with V+W (Table 2). Stressed mice treated with the cannabinoid agonist displayed an upregulation of *ApoE* ( $t(6)=6.48$ ;  $p_{adj}=0.05^*$ ) when compared to their non-stressed counterparts (Table 2). Socially defeat mice subjected to R+W showed elevated levels of *ApoE* ( $t(6)=9.18$ ;  $p_{adj}<0.001^{***}$ ), *Cnp* ( $t(6)=7.22$ ;  $p_{adj}<0.001^{***}$ ), *Vgf* ( $t(6)=8.35$ ;  $p_{adj}<0.001^{***}$ ), *Drd1* ( $t(6)=7.81$ ;  $p_{adj}<0.001^{***}$ ), *Drd5* ( $t(6)=5.95$ ;  $p_{adj}=0.02^*$ ), *Rxra* ( $t(6)=7.2$ ;  $p_{adj}<0.001^{***}$ ), *Zfp488* ( $t(6)=10.34$ ;  $p_{adj}<0.001^{***}$ ), *Mbp* ( $t(6)=6.92$ ;  $p_{adj}=0.01^{**}$ ), *Cnr1* ( $t(6)=6.51$ ;  $p_{adj}=0.02^*$ ), and *Ryr3* ( $t(6)=5.55$ ;  $p_{adj}=0.03^*$ ) in comparison to their counterparts non-exposed to stress (Table 2).

Table 2

Gene expression signature in the prefrontal cortex derived from control and stressed mice upon vehicle or cannabinoid drug exposure. Column titles from left to right: Comparison; Gene symbol; Accession; Fold Change; q-value. N= 4 mice per subgroup. CTR, control; STS, stress; V, vehicle; W, WIN55,212-2; R, rimonabant; q-value, adjusted p-value.

Comparison	Gene symbol	Accession	Fold change	q-value
STS V+W vs CTR V+W	<i>ApoE</i>	NM_009696.3	1.44	.01
	<i>CxCl12</i>	NM_001012477.2	1.54	.02
	<i>Dtnbp1</i>	NM_025772.4	1.36	.02
	<i>Ski</i>	NM_011385.2	1.46	.04
	<i>Cnr1</i>	NM_007726.3	1.63	.05
CTR R+W vs CTR V+W	<i>ApoE</i>	NM_009696.3	0.55	< .001
	<i>Rtn4r</i>	NM_022982.2	0.43	< .001
CTR R+W vs CTR V+W	<i>ApoE</i>	NM_009696.3	0.45	< .001
	<i>Rtn4r</i>	NM_022982.2	0.37	< .001
	<i>Vgf</i>	NM_001039385.1	0.46	.01
	<i>Rxra</i>	NM_011305.3	0.31	.01
	<i>Cnp</i>	NM_001146318.1	0.38	.02
	<i>Cnr1</i>	NM_007726.3	0.49	.03
	<i>Mbp</i>	NM_001025251.2	0.32	.05
STS V+W vs STS V+W	<i>Mag</i>	NM_010758.2	0.47	.04
STS R+V vs STS V+W	<i>ApoE</i>	NM_009696.3	0.80	.02
STS V+W vs CTR V+W	<i>ApoE</i>	NM_009696.3	1.40	.05
STS R+W vs CTR R+W	<i>ApoE</i>	NM_009696.3	2.23	.001
	<i>Cnp</i>	NM_001146318.1	3.03	.001
	<i>Vgf</i>	NM_001039385.1	2.44	.001
	<i>Drd1</i>	NM_010076.3	8.34	.001
	<i>Rxra</i>	NM_011305.3	3.28	.001
	<i>Zfp488</i>	NM_001013777.2	2.90	.001
	<i>Mbp</i>	NM_001025251.2	3.90	.01
	<i>Drd5</i>	NM_013503.2	4.18	.02

Comparison	Gene symbol	Accession	Fold change	q-value
	<i>Cnr1</i>	NM_007726.3	2.07	.02
	<i>Ryr3</i>	NM_177652.2	4.76	.03

## Pearson's chi-squared correlation analysis between gene expression and tubulin acetylation in the PFC

Administration of drugs had a consistent effect on tubulin acetylation in both control and stressed animals when the PFC was examined (Fig. 4). The administration of the inverse agonist led to a decrease in tubulin acetylation when compared to the control group treated with vehicle whereas the administration of either R+V or R+W reduced tubulin acetylation in contrast to what was observed upon W treatment. We, therefore, analyzed the correlation between tubulin acetylation and gene expression signature reporting an inverse association between acetylated tubulin levels and either *ApoE* ( $r=-0.94$ ;  $p<0.001^{***}$ ), *CxCl12 $\gamma$*  ( $r=-0.79$ ;  $p=0.019^*$ ), *Dtnbp1* ( $r=-0.79$ ;  $p=0.019^*$ ), *Ski* ( $r=-0.98$ ;  $p<0.001^{***}$ ) or *Cnr1* ( $r=-0.87$ ;  $p=0.005^{**}$ ) expression when comparing controls and defeat mice subjected to vehicle (Fig. 4, panel A); and also did so, after acute injection with V+W when compared the control and the stress group ( $r=-0.97$ ;  $p=0.001^{***}$ ) (Fig. 4, panel B). A positive correlation between acetylated tubulin and *ApoE* levels was reported following either V+W or R+V under repeated stress ( $r=0.74$ ;  $p=0.05^*$ ) (Fig. 4, panel C).

## Discussion

The dynamic rearrangement of the neuronal MTs is crucial for brain plasticity by enabling the remodelling of dendrites and axons<sup>43</sup>. Persistent stressful conditions revealed structural alterations of the cytoskeleton<sup>6,7</sup>. We asked here, whether psychosocial stress affects the neuronal cytoskeleton by investigating the post-translational tubulin modification based on the addition of acetyl groups. We found a significant reduction of tubulin acetylation in the PFC and the DS, whereas non-significant differences were observed in the HIPP and the CRB of mice exposed to chronic psychosocial stress. Reduced levels of tubulin acetylation in the PFC were accompanied by differential gene expression. Particularly, an upregulation of *ApoE*, *CxCl12 $\gamma$* , *Dtnbp1*, *Ski*, and *Cnr1* in the PFC of stressed mice was determined. The administration of V+W promoted an increase of both *ApoE* and *Cnr1* levels in comparison to R+W. Upregulation of *ApoE* was also observed in stressed mice treated with V+W in contrast to their matched controls. The data highlighted a consistent expression of *ApoE* deregulated by stress and also by the administration of the CB1 agonist which might indicate a CB1 mediated effect. Therefore, we investigated whether the administration of cannabinoid drugs might have a potential therapeutic effect to overcome the stress-induced cytoskeletal modifications.

Neuronal remodelling and brain plasticity are regulated by the MT system. In animals, stressful conditions can impair neuronal plasticity. Stress-induced neuronal atrophy in the HIPP by retraction of

apical dendrites, cell death, and decreased neurogenesis<sup>4,47-49</sup>. However, it is not restricted to this brain region. In particular, chronic restraint stress in experimental animals also provoked atrophy in the PFC<sup>46,50</sup>. Since acetylation of tubulin contributes to cytoskeletal stability, a decrease might lead to synaptic and dendrite alterations<sup>48</sup>. Consistently, we found a decreased tubulin acetylation in the PFC and the DS derived from mice exposed to psychosocial stress.

Our results indicate an imbalance of tubulin acetylation and deacetylation in social defeat mice pointing to either reduced expression or inhibition of the enzymatic activity of the acetyltransferase *Atat1* or hyperactivity of the HDAC6 tubulin deacetylase. A change in gene expression, neither for *Atat1* nor *Hdac6*, was not assessed by Nanostring gene expression arrays. However, it is well known that ATAT1 is highly expressed in the cerebral cortex and the HIPP (retrieved from The Human Protein Atlas at <https://www.proteinatlas.org/ENSG00000137343-ATAT1/tissue>), whereas HDAC6 is highly expressed in the brain and especially in the cortex, the HIPP, and the CRB<sup>(49)</sup>; retrieved from The Human Protein Atlas at <https://www.proteinatlas.org/ENSG00000094631-HDAC6/tissue>). Since HDAC6 is the main  $\alpha$ -tubulin deacetylase in the brain, changes in tubulin acetylation are most likely due to the deregulation of HDAC6 activity. HDAC6, additionally, targets also the chaperone Hsp90 and the redox regulatory proteins peroxiredoxin I and II (Prx I and II), both of them involved in the stress response<sup>21,50,51</sup>. Perturbation of acetylated tubulin dynamics has been reported in neuropsychiatric diseases and stress-related disorders<sup>8-10</sup>. Furthermore, HDAC6 affects the emotional behaviour of experimental animals since *Hdac6*-deficient mice exhibit hyperactivity, less anxiety, and anti-depressant-like behaviour<sup>27</sup>. Cells respond to stress immediately with the formation of cytoplasmic stress granules by recruitment of HDAC6. Interestingly, an appropriate activity of HDAC6 is required to counteract oxidative stress<sup>52</sup>. Besides that, HDAC6 is essential for the clearance of misfolded proteins and protein aggregates that are degraded by either the ubiquitin-proteasome pathway or autophagy. Indeed, HDAC6 binds to polyubiquitinated misfolded proteins favouring their retrograde MT transport to aggresomes. Thus, HDAC6 is a component of aggresomes that increases the efficiency and selectivity of autophagic degradation and protects cells from stress response caused by aggregation of misfolded proteins<sup>22,53</sup>. Subsequently, an increase of HDAC6 activity could promote autophagy and clearance of misfolded proteins and protein aggregates, e.g., aggregates of hyperphosphorylated Tau proteins generated by chronic stress<sup>6</sup>. A decrease in tubulin acetylation as observed in the PFC and the DS of the stress group could thus indicate a neuroprotective function attributable to the overactivation of HDAC6. Elevated levels of HDAC6 deacetylase activity are under the tight control of the kinases Aurora A and GSK3- $\beta$ <sup>54,55</sup>. Activation of Aurora A is regulated by HEF1 (human enhancer of filamentation 1) that in turn is activated by HIF-1 $\alpha$  (hypoxia-inducible factor 1 $\alpha$ )<sup>56</sup>. Thus, putatively, stressful events might induce hypoxic conditions that favour Aurora A and HDAC6 activation and lastly, tubulin deacetylation. Blockage of GSK3- $\beta$  inhibits deacetylase activity and simultaneously increases tubulin acetylation. GSK3- $\beta$  is a substrate of the PI3K/AKT pathway and becomes phosphorylated and inactivated by stimulation of AKT. Thus, the inhibition of the AKT pathway activates HDAC6 reducing tubulin acetylation. Additionally, GSK3- $\beta$  negatively regulates mitochondrial and anterograde axonal transport<sup>55,57</sup>. The activity of the PI3K/AKT pathway is controlled by upstream

molecules such as the CXCL12-CXCR4 and DTNBP1. Drug-induced tubulin acetylation and MT stabilization are suppressed upon CXCL12 activation in prostate cancer cells<sup>58</sup>. Dysbindin-1 regulates synapse morphology, synaptic plasticity, vesicle trafficking, and reduced dopamine-induced phosphorylation of AKT/GSK3 $\beta$ <sup>59</sup>. Thus, elevated levels of *Cxcl12* or *Dtnbp1*, as observed in the PFC of stressed animals, might contribute to HDAC6 hyperactivation and eventually tubulin deacetylation.

In the HIPp, the DS, and the CRB, activation of the G-protein coupled cannabinoid receptor CB1, by administration of  $\Delta$ 9-tetrahydrocannabinol (THC), increased phosphorylation of AKT, whereas the selective CB1 antagonist R blocked it<sup>60</sup>. Furthermore, the phosphorylation of GSK3- $\beta$  was also increased by THC administration<sup>60</sup>. We showed here, that the administration of the CB1 agonist increased tubulin acetylation in the PFC of stressed animals. In contrast, a reduction or no significant changes were found in the HIPp, the DS, and the CRB of the control and the stress group when the same drug was administered. As expected, activation of CB1 by use of the cannabinoid agonist activates AKT kinase that in turn inactivates GSK3- $\beta$  by phosphorylation eventually blocking the activity of HDAC6 resulting in elevated levels of tubulin acetylation. Such effect was observed exclusively in the PFC. We reported higher expression of *Cnr1* in the PFC of stressed animals that could prevent the hyperactivation of HDAC6 via PI3K/AKT signaling. Instead, we observed a decrease in tubulin acetylation levels pointing out that the overexpression of *Cnr1* measured here might act as a compensatory mechanism to counteract the reduced levels of tubulin acetylation. However, further analyses warrant investigation. Collectively, our results demonstrate that distinct brain regions respond differentially to either prolonged stress or the administration of cannabinoid drugs. Furthermore, the different levels of tubulin acetylation reported here could suggest that neuroprotection mediated by CB1 is quite variable and cell type-specific. In summary, our findings revealed a reduction of tubulin acetylation under chronic stress when the PFC and the DS were studied. This fact could be an indicator of HDAC6 hyperactivity. Dysfunctions in tubulin acetylation under stress conditions might indicate that cellular architecture and vesicle transport are compromised<sup>14,15</sup>. But taking into account the protective role of HDAC6 against cellular stress, an alternative scenario could suggest that changes in tubulin acetylation could confer protection against chronic stress instead of being just a detrimental outcome.

Chronic psychosocial stress, such as the social defeat model, caused a variety of molecular, physiological, and behavioral changes<sup>34,35,39</sup>. Upon repeated psychosocial stress, differential gene expression was found in the CRB and other brain regions<sup>35,61</sup>. Elevated levels of *ApoE*, *Cxcl12*, *Dtnbp1*, *Ski*, and *Cnr* were found in stressed mice subjected to V+V when compared to their matched controls (Table 2). As reported, most of these genes are related to neuronal functioning. ApoE is involved in lipid metabolism and acts as the principal cholesterol carrier in the brain<sup>62</sup>. Experimental and clinical studies both revealed that *ApoE* levels are related to stress response<sup>63,64</sup>. Furthermore, repeated psychosocial stress per se stimulates inflammatory response by activating leukocyte extravasation through the blood-brain barrier into the brain<sup>65</sup>. This process is tightly regulated by the complex *Cxcl12-Cxcr4*. Repeated social defeat promotes the synthesis of *Cxcl12* within the brain exacerbating the pro-inflammatory reaction<sup>66</sup> in line with the results reported here. *Dtnbp1* is involved in distinct biological processes,

including dendritic spines and synapse formation<sup>67</sup>. Overexpression of *Dtnbp1* under stress conditions might confer vulnerability to psychotropic drugs<sup>68</sup>. *Ski* is a transcriptional modulator required for the expansion of precursor cells in the neuroepithelium or skeletal muscle lineages<sup>69</sup>. *Ski* has been involved in distinct biological processes such as muscle homeostasis, axonal growth, myelination, hematopoietic cell differentiation, regulation of T-cells as well as in many complex pathologies<sup>70</sup>. However, its function in the context of prolonged stress remains to be elucidated and warrants further investigation.

The administration of both drugs reduced *ApoE* and *Rtn4r* levels when compared to those subjected to vehicle alone. Here, we demonstrated that alterations in the endocannabinoid signalling by either long-term stress or acute cannabinoid treatment are accompanied by changes in *ApoE* expression<sup>35,71</sup>. We reported elevated levels of *ApoE* in the control group after V+W injection in contrast to those treated with R+W. Similarly, Russell and colleagues (2010) found an increase of *ApoE* attributable to the drug W<sup>72</sup> while the antagonist acted oppositely<sup>73</sup>. *Rtn4r* encodes a glycosylphosphatidylinositol-anchored protein remarkably present in the PFC<sup>74</sup> that has been involved in oligodendrocyte proliferation<sup>75</sup>, cytoskeleton organization<sup>76</sup>, and neuronal processes such as neurotransmission, regeneration, sprouting, and plasticity<sup>77</sup>. A decrease in *Rtn4r* following R+W treatment was measured when compared to vehicle alone which might act as a compensatory mechanism against functional disruption of the neural PFC system. Indeed, elevated levels of *Rtn4r* compromise the proper function of PFC<sup>78</sup>. Acute administration of the cannabinoid agonist in non-stressed mice led to an overexpression of *Cnp* and *Mbp* when compared to those treated with R+W. CNP participates in RNA splicing, trafficking, and metabolism in mature oligodendrocytes<sup>79–82</sup>. In contrast, MBP regulates the adhesion of compact multilayered myelin sheath<sup>83</sup>. An increase in both myelin-related genes might indicate deficits in myelin CNS architecture<sup>78</sup>. Levels of *Vgf*, encoding a neuropeptide involved in energy balance, were higher following V+W treatment<sup>84</sup>, while the inverse agonist had the opposite effect<sup>85</sup>. This is in line with the results reported upon V+W administration in comparison to R+W. Interestingly, elevated levels of this neuropeptide exacerbated the inflammatory response in rodents<sup>86</sup>. Retinoic acid receptor RXR-alpha (*Rxra*) participates in the regulation of calcium signalling<sup>87</sup> and synapse formation<sup>88</sup>. Upon activation, RXRA stimulates oligodendrocyte differentiation<sup>89</sup> and promotes the phagocytic functions of microglia<sup>87</sup>. The data presented herein show elevated levels of *Rxra* following treatment with the CB1 agonist in contrast to R+W. We speculate that this might indicate dysfunctions in oligodendrocyte differentiation, synapse formation, and immune response. The expression of CB1 receptor, encoded by the *Cnr1* gene, was higher following V+W than when both drugs were administered in agreement with<sup>78</sup>.

Socially defeat mice treated with V+W exhibited lower expression of *Mag* in comparison to those subjected to vehicle alone. The overall differences observed between these groups could be attributable to the dosage of the cannabinoid agonist applied. An *in vitro* model of oligodendrocyte differentiation revealed that a low dosage of the cannabinoid agonist confers neuroprotection while the administration of higher doses of the drug aggravates demyelination<sup>90</sup>. Loss of *Mag*, encoding a transmembrane glycoprotein localized at peri-axonal regions of oligodendroglia, is associated with oligodendrocyte

dysfunctions<sup>91</sup>. Under stress conditions, intraperitoneal injection of the cannabinoid antagonist induced a reduction in *ApoE* levels in comparison to V+W. In contrast, stressed mice subjected to the cannabinoid agonist displayed higher expression of *ApoE* than their non-stressed counterparts which is in keeping with<sup>72</sup>. Socially defeat mice treated with both cannabinoid drugs underwent elevated levels of *ApoE*, *Cnp*, *Vgf*, *Drd1*, *Drd5*, *Rxra*, *Zfp488*, *Mbp*, *Cnr1*, and *Ryr3* in comparison to their non-stressed counterparts (Table 2). Mice subjected to chronic stress and acutely treated with both cannabinoid drugs showed elevated levels of *ApoE*<sup>71-73</sup>. Co-administration of both drugs under stress resulted in higher levels of *Vgf* which, in turn, could be attributable to the cannabinoid agonist W<sup>84</sup>. Indeed, exposure to either psychosocial stress or acute administration of the inverse agonist acted in the opposite direction than the cannabinoid agonist did<sup>85,92</sup>. Dopaminergic neurotransmission is essential for cerebral function, controlling various physiological mechanisms including cognition, locomotion, neuroendocrine activity, emotional and motivational aspects<sup>93</sup>. Recent studies have demonstrated that midbrain dopaminergic neurons are particularly vulnerable to microtubule disruptions<sup>94</sup>. We measured a prominent expression of *Drd5* in stressed mice subjected to R+W which could be explained by a stress-mediated effect<sup>95</sup> rather than the consumption of cannabinoid drugs<sup>96</sup>. The administration of R+W under the influence of stress resulted in more *Rxra* expression than in their non-stressed counterparts. Elevated levels of *Rxra* might be associated with the use of cannabinoid drugs<sup>35,97</sup>. There are no data available as yet on the role of *Rxra* in the context of chronic stress. Subsequently, the function of *Rxra* under repeated psychosocial stress warrants further investigation. The proliferation of oligodendrocyte precursor cells into myelinating oligodendrocytes is regulated by distinct transcription factors like ZFP488<sup>98</sup>. We reported an increase of *Zfp488* when socially defeat mice were subjected to both cannabinoids in comparison to their non-stressed counterparts<sup>99</sup>. This fact might indicate dysfunctions in oligodendrocyte differentiation<sup>98</sup>. Upon coadministration with R+W, stressed mice displayed higher *Mbp* expression than their control counterparts indicating perturbations in CNS myelination<sup>83</sup>. These alterations could be explained by the administration of synthetic cannabinoid drugs<sup>100</sup> rather than exposure to a repeated stressor<sup>101</sup>. The expression of *Cnr1* was higher in stressed mice subjected to R+W than their controls subjected to equal pharmacological treatment. Such increase could be attributed to either drug treatment<sup>102</sup> or exposure to chronic stress<sup>103</sup>. Ca<sup>2+</sup> release into the cytoplasm of neurons is regulated by ryanodine receptors<sup>104</sup>. Changes in RYR3 activity lead to an imbalance in intracellular levels of calcium contributing to an impairment in neurotransmission<sup>105</sup> and lastly neurodegeneration<sup>106</sup>. We reported higher expression of *Ryr3* in social defeat mice treated with R+W than their matched non-stressed mice. This evidence might be explained by either chronic exposure to a stressor<sup>107</sup> or acute cannabinoid administration<sup>108</sup>.

In summary, we concluded that the decrease in acetylated MTs most likely affects neurotransmission, which nevertheless could promote neuroprotection under long-term stress conditions. Additionally, enhanced HDAC6 activity attributable to lower levels of tubulin acetylation could promote autophagy and clearance of misfolded proteins and aggregates in stressed animals<sup>6</sup>. In this regard, we can speculate that an increase of *ApoE* under the influence of stress might contribute to neuroprotection as well. It has been shown that *ApoE* participates in MT polymerization and neurite extension<sup>109,110</sup>. HDAC6 affects

both the nuclear localization of ApoE and the microtubule-organizing center<sup>111</sup>. Thus, elevated levels of ApoE together with a decrease in tubulin acetylation might indicate a dynamic reassembling of the MTs. Collectively, the overexpression of *ApoE*, *Cxcl12*, *Dtnbp1*, and *Cnr1* in the PFC of stressed animals may trigger MT destabilization while tubulin deacetylation could promote MT reorganization acting as a protective mechanism against the side effects of stress. We found a consistent expression of *ApoE* attributable to either psychosocial stress<sup>63,64</sup> or administration of the CB1 agonist<sup>72</sup>. Interestingly, the expression of ApoE was inversely correlated with acetylated tubulin levels when comparing controls and stressed mice subjected to the CB1 agonist whereas the use of the CB1 inverse agonist acted oppositely. This fact might indicate a CB1 receptor-mediated effect. The diverse effects on tubulin acetylation observed in the studied brain regions of both control and stressed animals with or without pharmacological treatment might indicate that HDAC6 activity is differently regulated in the brain acting simultaneously on different cellular mechanisms to safeguard homeostatic processes for the proper function of the CNS.

## Materials And Methods

### Ethics statement

All procedures were approved by the Göttingen University Institutional Animal Care and Use Committee and were in accordance with NIH guidelines for the use of animals in research and the European Communities Council Directive (2010/63/EU). The study was designed and carried out in compliance with the ARRIVE guidelines.

### Psychosocial stress experiment

Male mice of strains C57Bl6/J and FVB/N were purchased from Charles River Laboratories (Sulzfeld, Germany) and maintained under standard conditions (12-hours light/dark cycle with 6:00/18:00 lights on/off, a room temperature of 21±2°C, and food and water ad libitum). Male C57Bl6/J mice, aged 7-8 weeks, were habituated for one week before being subjected either to the resident-intruder paradigm or left undisturbed as the control groups. One-year-old male FVB/N mice were kept individually and used as residents. For the social stress procedure, an intruder (C57Bl6/J mouse) was placed in the home cage of a resident (FVB/N mouse) where they freely interacted until first aggression took place. Afterward, the intruder was isolated within the resident's cage to prevent any further physical aggression but still subjected to odorous, visual, and vibrissae contact with the resident. The psychosocial stress protocol was performed one hour a day for 21 days. Control mice were placed in an empty cage once per day as their stressed counterparts did but without contact with FVB/N strain<sup>34</sup>.

### Drug treatments

The CB1 receptor agonist WIN55,212-2 (referred to in the text as W, Sigma-Aldrich, Seelze, Germany) and the selective cannabinoid CB1 inverse agonist rimonabant (referred to in the text as R, Sequoia Research Products Ltd., Pangbourne, UK) were dissolved in a vehicle solution consisting of 10% DMSO (Sigma-

Aldrich, Seelze, Germany) and 0.1% Tween-80 (Sigma-Aldrich, Seelze, Germany) in 0.9% saline. On day 21 of the experiment, the animals were injected intraperitoneally with a volume of 200  $\mu$ l of drug and/or vehicle. The drugs W and R were administered at a concentration of 3mg/kg. Control and stressed animals were split into four subgroups each that received different treatments. Mice were treated twice with vehicle (V+V) as the control group, or subjected first to the vehicle and then W (V+W), or treated first with R and then with W (R+W), or injected first with R and then with vehicle (R+V). Four mice per subgroup were used.

## Sample preparation

Animals were sacrificed immediately after finishing the experiment. All mice were deeply anesthetized by intraperitoneal injection of 2,2,2-tribromethanol (Sigma-Aldrich, Hamburg, Germany) followed by transcardial perfusion with cold 0.1% phosphate-buffered saline (PBS). Brain samples were isolated and frozen in liquid nitrogen. On the day of testing, tissues were homogenized in RIPA buffer containing protease inhibitors (Roche Applied Science, Penzberg, Germany). SDS-containing reducing sample buffer was added giving a final concentration of 1x<sup>112</sup>. Probes were denatured for 5 min at 60°C.

## Immuno-blotting

Protein lysates were separated on 10% SDS-polyacrylamide gels and transferred onto nitrocellulose membranes (AmershamHybond-ECL, GE Healthcare)<sup>112,113</sup>. The membrane was blocked in 5% dry milk in TBST (10 mM Tris-HCl pH 7.6, 150 mM NaCl, 0.05% Tween20) for one hour followed by incubation with the primary antibodies. These were mouse anti-acetylated  $\alpha$ -tubulin (clone 6-11B-1; Santa Cruz, #sc-23950), and rabbit anti- $\beta$ -actin (Proteintech, #20536-1-AP). Both antibodies were resuspended in blocking solution and incubated with the blots at 4°C overnight by constant agitation in roller tubes. Blots were washed for 30 minutes in TBST followed by incubation with fluorophore-labelled secondary antibodies goat anti-mouse IRDye800CW (LI-COR, #925-32210, lot #C81106-01), and goat anti-rabbit IRDye680RD (LI-COR, #925-68071, lot #C80911-11) for 45 minutes at room temperature in roller tubes. After 45 minutes of washing in TBST, fluorescent images were captured by Odyssey CLx Imaging System (LI-COR Biosciences, Nebraska, USA), and proteins were quantified using the software Image Studio<sup>TM</sup>Lite (LI-COR Biosciences, Nebraska, USA).

## Protein quantification

For comparative quantification, all probes were loaded onto four separate gels using four different biological replicates for each treatment, and immune-blotting and image capture were performed concurrently, using identical antibody dilutions, and identical image capture settings. Immune-blotting experiments were repeated several times giving a total of four biological replicates and up to five technical replicates for each probe. Relative quantification was obtained by calculating the ratio of acetylated tubulin versus  $\beta$ -actin in the same lane. The fold change of relative tubulin acetylation was determined using the mean of the relative tubulin acetylation of the four biological control probes (obtained from mice not subjected to psychosocial stress, and injected with vehicle only, CTR (V+V)) as the reference, which was set as 1. The fold changes were calculated for all probes investigated

concurrently on a set of four blots. The fold changes obtained from all replicates were finally assembled as presented in the pictures.

## Focused gene signature profiling

The prognostic 35-gene profile was performed in the digital transcript counting assay (nCounter-NanoString). The nCounter® technology permits the counting of individual nucleic acid molecules using digital detection of the fluorescent molecular barcodes attached to the target RNA. The mRNA hybridization, detection, and scanning were performed following the protocol provided by NanoString Technologies. 200–400 ng of RNA was taken as the starting material according to the manufacturer's guidelines. Data were adjusted by scaling with the geometric mean of built-in control gene probes after log transformation (base 2) for each sample. The target genes were chosen according to the following criteria: genes involved in cytoskeleton architecture, neuropsychiatric disorders, and CNS myelination. The NanoStringnCounter™ code set was assigned as follows: *β-actin* (NM\_007393.3), *apolipoprotein E (ApoE)* (NM\_009696.3), *C-X-C motif chemokine 12 (Cxcl12)* (NM\_001012477.2), *calreticulin (Calr)* (NM\_007591.3), *cannabinoid receptor 1 (Cnr1)* (NM\_007726.3), *cannabinoid receptor 2 (Cnr2)* (NM\_009924.3), *cub and sushi multiple domains 1 (Csm1)* (NM\_053171.2), *2',3'-cyclic nucleotide 3'-phosphodiesterase (Cnp)* (NM\_001146318.1), *diacylglycerol lipase (Dagl-α)* (NM\_198114.2), *discoidin domain receptor 1 (Ddr1)* (NM\_001198831.1), *dopamine receptor D1 (Drd1)* (NM\_010076.3), *dopamine receptor D2 (Drd2)* (NM\_010077.2), *dopamine receptor D3 (Drd3)* (NM\_007877.1), *dopamine receptor D4 (Drd4)* (NM\_007878.2), *dopamine receptor D5 (Drd5)* (NM\_013503.2), *dystrobrevin binding protein 1 (Dtnbp1)* (NM\_025772.4), *galactosylceramidase (Galc)* (NM\_008079.3), *glyceraldehyde-3-phosphate dehydrogenase (Gapdh)* (NM\_008084.2), *low density lipoprotein receptor (Ldlr)* (NM\_001252658.1), *myelin basic protein (Mbp)* (NM\_001025251.2), *myelin-associated glycoprotein (Mag)* (NM\_010758.2), *myelin oligodendrocyte glycoprotein (Mog)* (NM\_010814.2), *N-acyl phosphatidylethanolamine-specific phospholipase D (Nape-pld)* (NM\_178728.5), *nerve growth factor inducible (Vgf)* (NM\_001039385.1), *neuregulin 1 (Nrg1)* (NM\_178591.2), *oligodendrocyte transcription factor 1 (Olig1)* (NM\_016968.4), *oligodendrocyte transcription factor 2 (Olig2)* (NM\_016967.2), *reticulon 4 receptor (Rtn4r)* (NM\_022982.2), *retinoid X receptor alpha (Rxra)* (NM\_011305.3), *ryanodine receptor 3 (Ryr3)* (NM\_177652.2), *ski proto-oncogene (Ski)* (NM\_011385.2), *special AT-rich sequence-binding protein-2 (Satb2)* (NM\_139146.2), *SRY-box 10 (Sox10)* (NM\_011437.1), *zinc finger protein 488 (Zfp488)* (NM\_001013777.2), and *zinc finger protein GLI1 (Gli1)* (NM\_010296.2). The mean value of the expression levels of *Gapdh* and *β-actin* was used as the standard control. Four mice per subgroup were used.

## Statistical analysis

Pairwise comparisons between the controls and stressed animals and between specific drug treatment and the vehicle were evaluated by Student's t-test (unpaired, two-tailed). Excel was used to verify normal distribution of the data. A two-way ANOVA was used to determine the effects of long-term stress and drug treatment on the expression of acetylated tubulin. The mean differences among the levels of one factor were determined by one-way ANOVA. Pairwise comparisons were performed using Bonferroni post hoc test. Gene expression profile was determined as a two-tailed *t*-test on the log-transformed normalized

data that assumed unequal variance using nSolver™ 4.0. The distribution of the *t*-statistic was calculated using the Welch-Satterthwaite equation for the degrees of freedom in the estimation of the 95% confidence limits for observed differential expression between the two groups. Statistics and graphs were shown using GraphPad Prism 9.1.0. The resulting p-values were adjusted according to Benjamini-Hochberg<sup>114</sup>. The significance was set at  $p \leq 0.05$ . In all figures and text, data are represented as mean  $\pm$  SE.

## Declarations

### Acknowledgments

The research was supported by Deutsche Forschungsgemeinschaft [Grant CNMPB C1-6]. Dr. Tomas-Roig was supported by Deutsche Forschungsgemeinschaft Rückkehrstipendium [Grant TO 977/2-1]. We acknowledge support from the Open Access Publication Funds of the Göttingen University.

### Author contributions

J.T.R. and S.H.F. initiated the study and designed the experiment. S. S. R, D.Z., and U.H.R. technically supported J.T.R. and S.H.F. J.T.R. and S.H.F. performed Nanostring NCounter analysis and Western blotting. J.T.R. and S.H.F. were responsible for the analysis of the data and wrote the manuscript. S.H.F., J.T.R., S. S. R, D.Z., and U.H.R. contributed to the discussion and reviewing, and editing of the manuscript.

### Competing interests

The authors declare no competing interests.

## References

1. van Os, J., Kenis, G. & Rutten, B. P. F. The environment and schizophrenia. *Nature* **468**, 203–212 (2010).
2. Uno, H., Tarara, R., Else, J. G., Suleman, M. A. & Sapolsky, R. M. Hippocampal damage associated with prolonged and fatal stress in primates. *J. Neurosci.* **9**, 1705–1711 (1989).
3. Gould, E., Tanapat, P., McEwen, B. S., Flügge, G. & Fuchs, E. Proliferation of granule cell precursors in the dentate gyrus of adult monkeys is diminished by stress. *Proc. Natl. Acad. Sci. U. S. A.* **95**, 3168–3171 (1998).
4. Magariños, A. M., Verdugo, J. M. G. & McEwen, B. S. Chronic stress alters synaptic terminal structure in hippocampus. *Proc. Natl. Acad. Sci.* **94**, 14002 LP – 14008 (1997).
5. Radley, J. J., Arias, C. M. & Sawchenko, P. E. Regional differentiation of the medial prefrontal cortex in regulating adaptive responses to acute emotional stress. *J. Neurosci.* **26**, 12967–12976 (2006).
6. Lopes, S. *et al.* Tau protein is essential for stress-induced brain pathology. *Proc. Natl. Acad. Sci. U. S. A.* **113**, E3755-63 (2016).

7. McEwen, B. S. *et al.* Mechanisms of stress in the brain. *Nat. Neurosci.* **18**, 1353–1363 (2015).
8. Wong, G. T.-H., Chang, R. C.-C. & Law, A. C.-K. A breach in the scaffold: the possible role of cytoskeleton dysfunction in the pathogenesis of major depression. *Ageing Res. Rev.* **12**, 67–75 (2013).
9. Marchisella, F., Coffey, E. T. & Hollos, P. Microtubule and microtubule associated protein anomalies in psychiatric disease. *Cytoskeleton (Hoboken)*. **73**, 596–611 (2016).
10. Kapitein, L. C. & Hoogenraad, C. C. Which way to go? Cytoskeletal organization and polarized transport in neurons. *Mol. Cell. Neurosci.* **46**, 9–20 (2011).
11. Verhey, K. J. & Gaertig, J. The tubulin code. *Cell Cycle* **6**, 2152–2160 (2007).
12. Garnham, C. P. & Roll-Mecak, A. The chemical complexity of cellular microtubules: tubulin post-translational modification enzymes and their roles in tuning microtubule functions. *Cytoskeleton (Hoboken)*. **69**, 442–463 (2012).
13. Janke, C. The tubulin code: molecular components, readout mechanisms, and functions. *J. Cell Biol.* **206**, 461–472 (2014).
14. Howes, S. C., Alushin, G. M., Shida, T., Nachury, M. V & Nogales, E. Effects of tubulin acetylation and tubulin acetyltransferase binding on microtubule structure. *Mol. Biol. Cell* **25**, 257–266 (2014).
15. Even, A. *et al.* ATAT1-enriched vesicles promote microtubule acetylation via axonal transport. *Sci. Adv.* **5**, eaax2705 (2019).
16. Kalebic, N. *et al.*  $\alpha$ TAT1 is the major  $\alpha$ -tubulin acetyltransferase in mice. *Nat. Commun.* **4**, 1962 (2013).
17. Kim, G.-W., Li, L., Ghorbani, M., You, L. & Yang, X.-J. Mice lacking  $\alpha$ -tubulin acetyltransferase 1 are viable but display  $\alpha$ -tubulin acetylation deficiency and dentate gyrus distortion. *J. Biol. Chem.* **288**, 20334–20350 (2013).
18. Li, L. *et al.* ATAT1 regulates forebrain development and stress-induced tubulin hyperacetylation. *Cell. Mol. Life Sci.* **76**, 3621–3640 (2019).
19. Hubbert, C. *et al.* HDAC6 is a microtubule-associated deacetylase. *Nature* **417**, 455–458 (2002).
20. North, B. J., Marshall, B. L., Borra, M. T., Denu, J. M. & Verdin, E. The human Sir2 ortholog, SIRT2, is an NAD<sup>+</sup>-dependent tubulin deacetylase. *Mol. Cell* **11**, 437–444 (2003).
21. Bobrowska, A., Donmez, G., Weiss, A., Guarente, L. & Bates, G. SIRT2 ablation has no effect on tubulin acetylation in brain, cholesterol biosynthesis or the progression of Huntington's disease phenotypes in vivo. *PLoS One* **7**, e34805 (2012).
22. Kawaguchi, Y. *et al.* The deacetylase HDAC6 regulates aggresome formation and cell viability in response to misfolded protein stress. *Cell* **115**, 727–738 (2003).
23. Hook, S. S., Orian, A., Cowley, S. M. & Eisenman, R. N. Histone deacetylase 6 binds polyubiquitin through its zinc finger (PAZ domain) and copurifies with deubiquitinating enzymes. *Proc. Natl. Acad. Sci. U. S. A.* **99**, 13425–13430 (2002).

24. Lee, J.-Y. *et al.* HDAC6 controls autophagosome maturation essential for ubiquitin-selective quality-control autophagy. *EMBO J.* **29**, 969–980 (2010).
25. Yan, J. Interplay between HDAC6 and its interacting partners: essential roles in the aggresome-autophagy pathway and neurodegenerative diseases. *DNA Cell Biol.* **33**, 567–580 (2014).
26. Odagiri, S. *et al.* Brain expression level and activity of HDAC6 protein in neurodegenerative dementia. *Biochem. Biophys. Res. Commun.* **430**, 394–399 (2013).
27. Fukada, M. *et al.* Loss of deacetylation activity of Hdac6 affects emotional behavior in mice. *PLoS One* **7**, e30924 (2012).
28. Liu, R. *et al.* SIRT2 is involved in the modulation of depressive behaviors. *Sci. Rep.* **5**, 8415 (2015).
29. Pandey, U. B. *et al.* HDAC6 rescues neurodegeneration and provides an essential link between autophagy and the UPS. *Nature* **447**, 859–863 (2007).
30. Esteves, A. R. *et al.* Acetylation as a major determinant to microtubule-dependent autophagy: Relevance to Alzheimer's and Parkinson disease pathology. *Biochim. Biophys. Acta. Mol. Basis Dis.* **1865**, 2008–2023 (2019).
31. Fuchikami, M. *et al.* The potential use of histone deacetylase inhibitors in the treatment of depression. *Prog. Neuropsychopharmacol. Biol. Psychiatry* **64**, 320–324 (2016).
32. Turu, G. & Hunyady, L. Signal transduction of the CB1 cannabinoid receptor. *J. Mol. Endocrinol.* **44**, 75–85 (2010).
33. Ladarre, D., Roland, A. B., Biedzinski, S., Ricobaraza, A. & Lenkei, Z. Polarized cellular patterns of endocannabinoid production and detection shape cannabinoid signaling in neurons. *Front. Cell. Neurosci.* **8**, 426 (2014).
34. Tomas-Roig, J. *et al.* Effects of repeated long-term psychosocial stress and acute cannabinoid exposure on mouse corticostriatal circuitries: Implications for neuropsychiatric disorders. *CNS Neurosci. Ther.* **24**, (2018).
35. Tomas-Roig, J. & Havemann-Reinecke, U. Gene expression signature in brain regions exposed to long-term psychosocial stress following acute challenge with cannabinoid drugs. *Psychoneuroendocrinology* **102**, (2019).
36. Bénard, G. *et al.* Mitochondrial CB<sub>1</sub> receptors regulate neuronal energy metabolism. *Nat. Neurosci.* **15**, 558–564 (2012).
37. English, J. A., Dicker, P., Föcking, M., Dunn, M. J. & Cotter, D. R. 2-D DIGE analysis implicates cytoskeletal abnormalities in psychiatric disease. *Proteomics* **9**, 3368–3382 (2009).
38. Piubelli, C., Carboni, L., Becchi, S., Mathé, A. A. & Domenici, E. Regulation of cytoskeleton machinery, neurogenesis and energy metabolism pathways in a rat gene-environment model of depression revealed by proteomic analysis. *Neuroscience* **176**, 349–380 (2011).
39. Tomas-Roig, J. *et al.* Social defeat leads to changes in the endocannabinoid system: An overexpression of calreticulin and motor impairment in mice. *Behav. Brain Res.* **303**, (2016).

40. Duval, E. R., Javanbakht, A. & Liberzon, I. Neural circuits in anxiety and stress disorders: A focused review. *Therapeutics and Clinical Risk Management* vol. 11 115–126 (2015).
41. Blair, K. S. *et al.* Atypical modulation of medial prefrontal cortex to self-referential comments in generalized social phobia. *Psychiatry Res. - Neuroimaging* **193**, 38–45 (2011).
42. Sripada, C., Angstadt, M., Liberzon, I., McCabe, K. & Phan, K. L. Aberrant reward center response to partner reputation during a social exchange game in generalized social phobia. *Depress. Anxiety* **30**, 353–361 (2013).
43. Pittenger, C. & Duman, R. S. Stress, depression, and neuroplasticity: a convergence of mechanisms. *Neuropsychopharmacol. Off. Publ. Am. Coll. Neuropsychopharmacol.* **33**, 88–109 (2008).
44. McEwen, B. S. Stress and hippocampal plasticity. *Annu. Rev. Neurosci.* **22**, 105–122 (1999).
45. Duman, R. S., Malberg, J., Nakagawa, S. & D'Sa, C. Neuronal plasticity and survival in mood disorders. *Biol. Psychiatry* **48**, 732–739 (2000).
46. Bianchi, M., Heidbreder, C. & Crespi, F. Cytoskeletal changes in the hippocampus following restraint stress: role of serotonin and microtubules. *Synapse* **49**, 188–194 (2003).
47. Radley, J. J. *et al.* Repeated stress induces dendritic spine loss in the rat medial prefrontal cortex. *Cereb. Cortex* **16**, 313–320 (2006).
48. Janke, C. & Montagnac, G. Causes and Consequences of Microtubule Acetylation. *Curr. Biol.* **27**, R1287–R1292 (2017).
49. Broide, R. S. *et al.* Distribution of histone deacetylases 1-11 in the rat brain. *J. Mol. Neurosci.* **31**, 47–58 (2007).
50. Kovacs, J. J. *et al.* HDAC6 regulates Hsp90 acetylation and chaperone-dependent activation of glucocorticoid receptor. *Mol. Cell* **18**, 601–607 (2005).
51. Parmigiani, R. B. *et al.* HDAC6 is a specific deacetylase of peroxiredoxins and is involved in redox regulation. *Proc. Natl. Acad. Sci. U. S. A.* **105**, 9633–9638 (2008).
52. Kwon, S., Zhang, Y. & Matthias, P. The deacetylase HDAC6 is a novel critical component of stress granules involved in the stress response. *Genes Dev.* **21**, 3381–3394 (2007).
53. Iwata, A., Riley, B. E., Johnston, J. A. & Kopito, R. R. HDAC6 and microtubules are required for autophagic degradation of aggregated huntingtin. *J. Biol. Chem.* **280**, 40282–40292 (2005).
54. Pugacheva, E. N., Jablonski, S. A., Hartman, T. R., Henske, E. P. & Golemis, E. A. HEF1-dependent Aurora A activation induces disassembly of the primary cilium. *Cell* **129**, 1351–1363 (2007).
55. Chen, S., Owens, G. C., Makarenkova, H. & Edelman, D. B. HDAC6 regulates mitochondrial transport in hippocampal neurons. *PLoS One* **5**, e10848 (2010).
56. Kim, S.-H. *et al.* Human enhancer of filamentation 1 is a mediator of hypoxia-inducible factor-1 $\alpha$ -mediated migration in colorectal carcinoma cells. *Cancer Res.* **70**, 4054–4063 (2010).
57. Morfini, G., Szebenyi, G., Elluru, R., Ratner, N. & Brady, S. T. Glycogen synthase kinase 3 phosphorylates kinesin light chains and negatively regulates kinesin-based motility. *EMBO J.* **21**, 281–293 (2002).

58. Bhardwaj, A. *et al.* CXCL12/CXCR4 signaling counteracts docetaxel-induced microtubule stabilization via p21-activated kinase 4-dependent activation of LIM domain kinase 1. *Oncotarget* **5**, 11490–11500 (2014).
59. Wang, H., Xu, J., Lazarovici, P. & Zheng, W. Dysbindin-1 Involvement in the Etiology of Schizophrenia. *Int. J. Mol. Sci.* **18**, (2017).
60. Ozaita, A., Puighermanal, E. & Maldonado, R. Regulation of PI3K/Akt/GSK-3 pathway by cannabinoids in the brain. *J. Neurochem.* **102**, 1105–1114 (2007).
61. Tomas-Roig, J. *et al.* Social defeat leads to changes in the endocannabinoid system: An overexpression of calreticulin and motor impairment in mice. *Behav Brain Res* **303**, 34–43 (2016).
62. Puglielli, L., Tanzi, R. E. & Kovacs, D. M. Alzheimer's disease: the cholesterol connection. *Nat. Neurosci.* **6**, 345–351 (2003).
63. Cameron, B. M., VanderPutten, D. M. & Merrill, C. R. Preliminary study of an increase of a plasma apolipoprotein E variant associated with peripheral nerve damage. A finding in patients with chronic spinal pain. *Spine (Phila. Pa. 1976)*. **20**, 581–590 (1995).
64. Gordon, I., Ben-Eliyahu, S., Rosenne, E., Sehayek, E. & Michaelson, D. M. Derangement in stress response of apolipoprotein E-deficient mice. *Neurosci. Lett.* **206**, 212–214 (1996).
65. Miller, A. H., Maletic, V. & Raison, C. L. Inflammation and its discontents: the role of cytokines in the pathophysiology of major depression. *Biol. Psychiatry* **65**, 732–741 (2009).
66. Sawicki, C. M. *et al.* Social defeat promotes a reactive endothelium in a brain region-dependent manner with increased expression of key adhesion molecules, selectins and chemokines associated with the recruitment of myeloid cells to the brain. *Neuroscience* **302**, 151–164 (2015).
67. Huang, C. C. Y., Muszynski, K. J., Bolshakov, V. Y. & Balu, D. T. Deletion of Dtnbp1 in mice impairs threat memory consolidation and is associated with enhanced inhibitory drive in the amygdala. *Transl. Psychiatry* **9**, 132 (2019).
68. *Modeling the Psychopathological Dimensions of Schizophrenia From Molecules to Behavior.* (ScienceDirect, 2016).
69. Berk, M., Desai, S. Y., Heyman, H. C. & Colmenares, C. Mice lacking the ski proto-oncogene have defects in neurulation, craniofacial, patterning, and skeletal muscle development. *Genes Dev.* **11**, 2029–2039 (1997).
70. Deheuninck, J. & Luo, K. Ski and SnoN, potent negative regulators of TGF-beta signaling. *Cell Res.* **19**, 47–57 (2009).
71. Bartelt, A. *et al.* Altered endocannabinoid signalling after a high-fat diet in Apoe <sup>-/-</sup> mice: Relevance to adipose tissue inflammation, hepatic steatosis and insulin resistance. *Diabetologia* **54**, 2900–2910 (2011).
72. Russell, J. C. *et al.* Rimonabant-mediated changes in intestinal lipid metabolism and improved renal vascular dysfunction in the JCR:LA-cp rat model of prediabetic metabolic syndrome. *Am. J. Physiol. Gastrointest. Liver Physiol.* **299**, G507-16 (2010).

73. Babenko, V. N., Smagin, D. A. & Kudryavtseva, N. N. RNA-Seq Mouse Brain Regions Expression Data Analysis: Focus on ApoE Functional Network. *J. Integr. Bioinform.* **0**, (2017).
74. Josephson, A. *et al.* Nogo-receptor gene activity: cellular localization and developmental regulation of mRNA in mice and humans. *J. Comp. Neurol.* **453**, 292–304 (2002).
75. Mi, S. *et al.* LINGO-1 negatively regulates myelination by oligodendrocytes. *Nat. Neurosci.* **8**, 745–751 (2005).
76. Petratos, S., Azari, M. F., Ozturk, E., Papadopoulos, R. & Bernard, C. C. a. Novel therapeutic targets for axonal degeneration in multiple sclerosis. *J. Neuropathol. Exp. Neurol.* **69**, 323–34 (2010).
77. Akbik, F., Cafferty, W. B. J. & Strittmatter, S. M. Myelin associated inhibitors: a link between injury-induced and experience-dependent plasticity. *Exp. Neurol.* **235**, 43–52 (2012).
78. Tomas-Roig, J., Wirths, O., Salinas-Riester, G. & Havemann-Reinecke, U. The Cannabinoid CB1/CB2 Agonist WIN55212.2 Promotes Oligodendrocyte Differentiation In Vitro and Neuroprotection During the Cuprizone-Induced Central Nervous System Demyelination. *CNS Neurosci Ther* (2016) doi:doi: 10.1111/cns.12506.
79. Bifulco, M., Laezza, C., Stingo, S. & Wolff, J. 2',3'-Cyclic nucleotide 3'-phosphodiesterase: a membrane-bound, microtubule-associated protein and membrane anchor for tubulin. *Proc. Natl. Acad. Sci. U. S. A.* **99**, 1807–1812 (2002).
80. Gobert, R. P. *et al.* Convergent functional genomics of oligodendrocyte differentiation identifies multiple autoinhibitory signaling circuits. *Mol. Cell. Biol.* **29**, 1538–1553 (2009).
81. Gravel, M. *et al.* 2',3'-Cyclic nucleotide 3'-phosphodiesterase: A novel RNA-binding protein that inhibits protein synthesis. *J. Neurosci. Res.* **87**, 1069–1079 (2009).
82. Lee, J., Gravel, M., Zhang, R., Thibault, P. & Braun, P. E. Process outgrowth in oligodendrocytes is mediated by CNP, a novel microtubule assembly myelin protein. *J. Cell Biol.* **170**, 661–673 (2005).
83. Boggs, J. M. Myelin basic protein: a multifunctional protein. *Cell. Mol. Life Sci.* **63**, 1945–1961 (2006).
84. Velasco, L., Ruiz, L., Sánchez, M. G. & Díaz-Laviada, I. delta(9)-Tetrahydrocannabinol increases nerve growth factor production by prostate PC-3 cells. Involvement of CB1 cannabinoid receptor and Raf-1. *Eur. J. Biochem.* **268**, 531–535 (2001).
85. Crunelle, C. L. *et al.* Cannabinoid-1 receptor antagonist rimonabant (SR141716) increases striatal dopamine D2 receptor availability. *Addict. Biol.* **18**, 908–911 (2013).
86. Soliman, N., Okuse, K. & Rice, A. S. C. VGF: a biomarker and potential target for the treatment of neuropathic pain? *Pain reports* **4**, e786 (2019).
87. Ting, S.-M. *et al.* Brain Cleanup as a Potential Target for Poststroke Recovery: The Role of RXR (Retinoic X Receptor) in Phagocytes. *Stroke* **51**, 958–966 (2020).
88. Cao, H. *et al.* Retinoid X Receptor  $\alpha$  Regulates DHA-Dependent Spinogenesis and Functional Synapse Formation In Vivo. *Cell Rep.* **31**, 107649 (2020).

89. Huang, J. K. *et al.* Retinoid X receptor gamma signaling accelerates CNS remyelination. *Nat. Neurosci.* **14**, 45–53 (2011).
90. Tomas-Roig, J. *et al.* Dose-dependent effect of cannabinoid WIN-55,212-2 on myelin repair following a demyelinating insult. *Sci. Rep.* **10**, (2020).
91. Lucchinetti, C. F., Brück, W., Rodriguez, M. & Lassmann, H. Distinct patterns of multiple sclerosis pathology indicates heterogeneity on pathogenesis. *Brain Pathol.* **6**, 259–274 (1996).
92. Jiang, C. *et al.* VGF function in depression and antidepressant efficacy. *Mol. Psychiatry* **23**, 1632–1642 (2018).
93. Alves, L. Q., Alves, J., Ribeiro, R., Ruivo, R. & Castro, F. The dopamine receptor D(5) gene shows signs of independent erosion in toothed and baleen whales. *PeerJ* **7**, e7758 (2019).
94. Yang, Y. *et al.* Stably maintained microtubules protect dopamine neurons and alleviate depression-like behavior after intracerebral hemorrhage. *Sci. Rep.* **8**, 12647 (2018).
95. Barko, K., Paden, W., Cahill, K. M., Seney, M. L. & Logan, R. W. Sex-Specific Effects of Stress on Mood-Related Gene Expression. *Mol. neuropsychiatry* **5**, 162–175 (2019).
96. Yanovich, C., Kirby, M. L., Michaelevski, I., Yadid, G. & Pinhasov, A. Social rank-associated stress vulnerability predisposes individuals to cocaine attraction. *Sci. Rep.* **8**, 1759 (2018).
97. Mukhopadhyay, B. *et al.* Transcriptional regulation of cannabinoid receptor-1 expression in the liver by retinoic acid acting via retinoic acid receptor-gamma. *J. Biol. Chem.* **285**, 19002–19011 (2010).
98. Biswas, S., Chung, S. H., Jiang, P., Dehghan, S. & Deng, W. Development of glial restricted human neural stem cells for oligodendrocyte differentiation in vitro and in vivo. *Sci. Rep.* **9**, 9013 (2019).
99. Xapelli, S. *et al.* Modulation of subventricular zone oligodendrogenesis: a role for hemopressin? *Front. Cell. Neurosci.* **8**, 1–9 (2014).
100. Tomas-Roig, J., Wirths, O., Salinas-Riester, G. & Havemann-Reinecke, U. The Cannabinoid CB1/CB2 Agonist WIN55212.2 Promotes Oligodendrocyte Differentiation In Vitro and Neuroprotection During the Cuprizone-Induced Central Nervous System Demyelination. *CNS Neurosci. Ther.* **22**, (2016).
101. Miguel-Hidalgo, J. J., Carter, K., Deloach, P. H., Sanders, L. & Pang, Y. Glucocorticoid-Induced Reductions of Myelination and Connexin 43 in Mixed Central Nervous System Cell Cultures Are Prevented by Mifepristone. *Neuroscience* **411**, 255–269 (2019).
102. Laprairie, R. B., Kelly, M. E. M. & Denovan-Wright, E. M. The dynamic nature of type 1 cannabinoid receptor (CB(1) ) gene transcription. *Br. J. Pharmacol.* **167**, 1583–95 (2012).
103. Bortolato, M. *et al.* Antidepressant-like activity of the fatty acid amide hydrolase inhibitor URB597 in a rat model of chronic mild stress. *Biol. Psychiatry* **62**, 1103–1110 (2007).
104. Liu, X. *et al.* Role of leaky neuronal ryanodine receptors in stress- induced cognitive dysfunction. *Cell* **150**, 1055–1067 (2012).
105. Fitzjohn, S. M. & Collingridge, G. L. Calcium stores and synaptic plasticity. *Cell Calcium* **32**, 405–411 (2002).
106. Mattson, M. P. Calcium and neurodegeneration. *Aging Cell* **6**, 337–350 (2007).

107. Nakamura-Maruyama, E. *et al.* Ryanodine receptors are involved in the improvement of depression-like behaviors through electroconvulsive shock in stressed mice. *Brain Stimul.* **14**, 36–47 (2021).
108. Isokawa, M. & Alger, B. E. Ryanodine receptor regulates endogenous cannabinoid mobilization in the hippocampus. *J. Neurophysiol.* **95**, 3001–3011 (2006).
109. Scott, B. L. *et al.* Human apolipoprotein E accelerates microtubule polymerization in vitro. *Neurosci. Lett.* **245**, 105–108 (1998).
110. Jiang, Q. *et al.* ApoE promotes the proteolytic degradation of Aβ. *Neuron* **58**, 681–693 (2008).
111. Balmik, A. A., Sonawane, S. K. & Chinnathambi, S. Modulation of Actin network and Tau phosphorylation by HDAC6 ZnF UBP domain. *bioRxiv* 702571 (2019) doi:10.1101/702571.
112. Laemmli, U. K. Cleavage of structural proteins during the assembly of the head of bacteriophage T4. *Nature* **227**, 680–685 (1970).
113. Towbin, H., Staehelin, T. & Gordon, J. Electrophoretic transfer of proteins from polyacrylamide gels to nitrocellulose sheets: procedure and some applications. *Proc. Natl. Acad. Sci. U. S. A.* **76**, 4350–4354 (1979).
114. Benjamini, Y. & Hochberg, Y. Controlling the False Discovery Rate: A Practical and Powerful Approach to Multiple Testing. *J. R. Stat. Soc. Ser. B* **57**, 289–300 (1995).

## Figures

### Figure 1

Psychosocial stress affects α-tubulin acetylation at K40 in different brain regions. Individual brain regions of control and stressed animals exposed to V+V were dissected and protein lysates prepared. Four biological replicates with several technical replicates were loaded onto SDS-gels, blotted, and finally tested with antibodies against acetylated-α-tubulin (K40) and β-actin. The relative amount of acetylated-α-tubulin was calculated by normalization for β-actin. The fold changes of acetylated-α-tubulin in distinct brain regions of stressed animals were calculated using the mean value of acetylated-α-tubulin in control animals as reference. Replicates (n): n=18 (PFC, CTR, V+V), n=18 (PFC, STS, V+V), n=16 (HIPP, CTR, V+V), n=23 (HIPP, STS, V+V), n=21 (DS, CTR, V+V), n=16 (DS, STS, V+V), n=18 (CRB, CTR, V+V), n=17 (CRB, STS, V+V). Light grey bars represent the stress group. CTR, control; STS, stress; V, vehicle; PFC, prefrontal cortex; HIPP, hippocampus; DS, dorsal striatum; CRB, cerebellum. One, two or three symbols indicate  $p < 0.05$ ;  $p < 0.01$ ,  $p < 0.001$ , respectively.

**Figure 2**

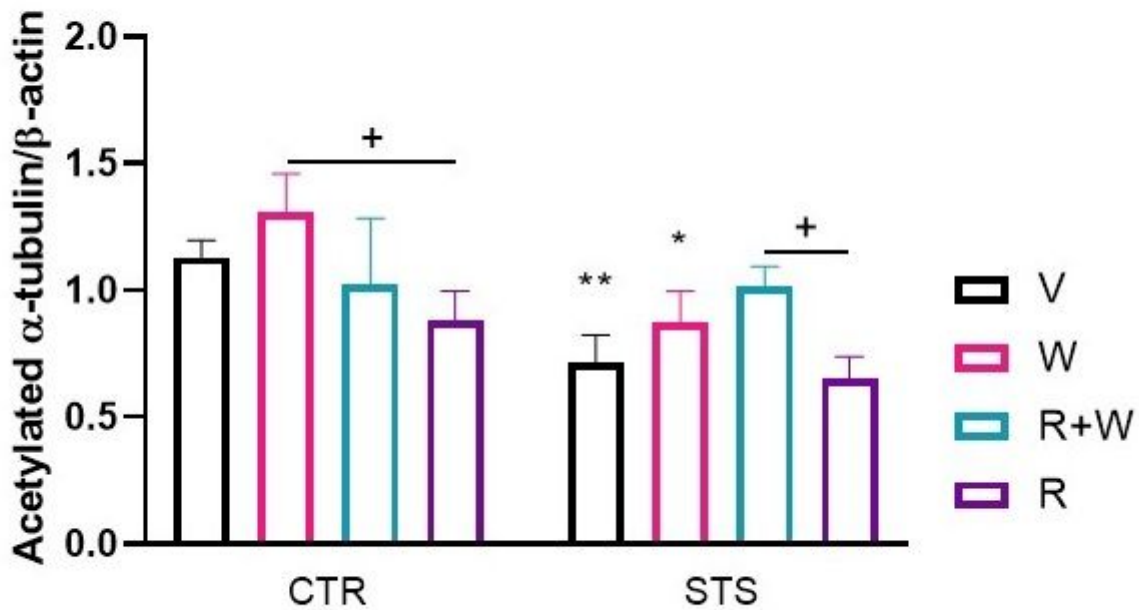


**Figure 2**

Effect of drug treatments on tubulin acetylation at K40 in the prefrontal cortex of stressed and non-stressed animals. We found higher expression of acetylated tubulin in controls treated with either V+V or V+W when compared to their stressed counterparts. The use of V+W in controls increased the expression of acetylated tubulin in contrast to the control group treated with R+V and also did so when both drugs were administered simultaneously under stress conditions in comparison with those subjected to stress and treated with R+V. Replicates (n): n=15 (CTR, V+V), n=17 (CTR, W+V), n=18 (CTR, W+R), n=19 (CTR, R+V), n=15 (STS, V+V), n=18 (STS, W+V), n=18 (STS, W+R), n=20 (STS, R+V). An \* indicates significant differences between controls exposed to cannabinoid drugs and their respective V+V control group. Intragroup comparisons between drug-treated mice are indicated by an underlined +. Otherwise underlined \* pointed out significant comparisons between stressed mice and their matched counterparts. CTR, control; STS, stress; V, vehicle; W, WIN55212.2; R, rimonabant. One, two or three symbols indicate  $P < 0.05$ ;  $P < 0.01$ ,  $P < 0.001$ , respectively.

**Figure 3**

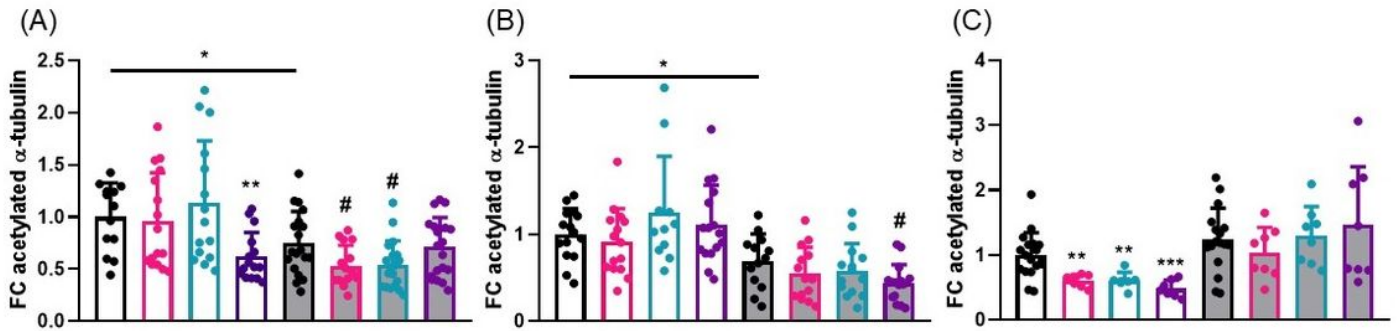


**Figure 3**

Psychosocial stress and cannabinoid drugs alter acetylation of  $\alpha$ -tubulin at K40 in distinct brain regions. (A) We found a significant reduction of tubulin acetylation in the hippocampus from control animals following R+V and also did so in stressed animals subjected to V+V when compared to controls V+V. Administration of either V+WIN or W+R in stressed animals led to a decrease of tubulin acetylation in comparison to stressed animals exposed to V+V whereas R+V under stress did not alter tubulin acetylation. Replicates (n): n=13(CTR, V+V), n=16(CTR, W+V), n=15(CTR, W+R), n=15(CTR, R+V), n=13(STS, V+V), n=15(STS, W+V), n=19(STS, W+R), n=20(STS, R+V). (B) In the dorsal striatum, we measured a reduction of tubulin acetylation in stressed animals exposed to V+V in comparison to their matched controls and also did so when stressed animals were treated with R+V in comparison to stressed animals subjected to V+V. Replicates (n): n=15(CTR, V+V), n=15(CTR, W+V), n=11(CTR, W+R), n=16(CTR, R+V), n=13(STS, V+V), n=14(STS, W+V), n=14(STS, W+R), n=16(STS, R+V). (C) In the cerebellum, the administration of cannabinoid drugs in controls caused a reduction in tubulin acetylation in comparison to controls subjected to V+V. Replicates (n): n=18(CTR, V+V), n=8(CTR, W+V), n=7(CTR, W+R), n=7(CTR, R+V), n=17(STS, V+V), n=8(STS, W+V), n=8(STS, W+R), n=8(STS, R+V). Light grey bars represent the stress group. An \* indicates significant differences between controls exposed to cannabinoid drugs and their respective V+V control group. An # indicates significant differences between stressed mice exposed to cannabinoid drugs and their respective V+V stress group. Intragroup comparisons between drug-treated mice are indicated by an underlined +. Otherwise underlined \* pointed out significant comparisons between stressed mice and their matched counterparts. CTR, control; STS, stress; V, vehicle; W, WIN55,212-2; R, rimonabant. One, two or three symbols indicate  $P < 0.05$ ;  $P < 0.01$ ,  $P < 0.001$ , respectively.

**Figure 4**

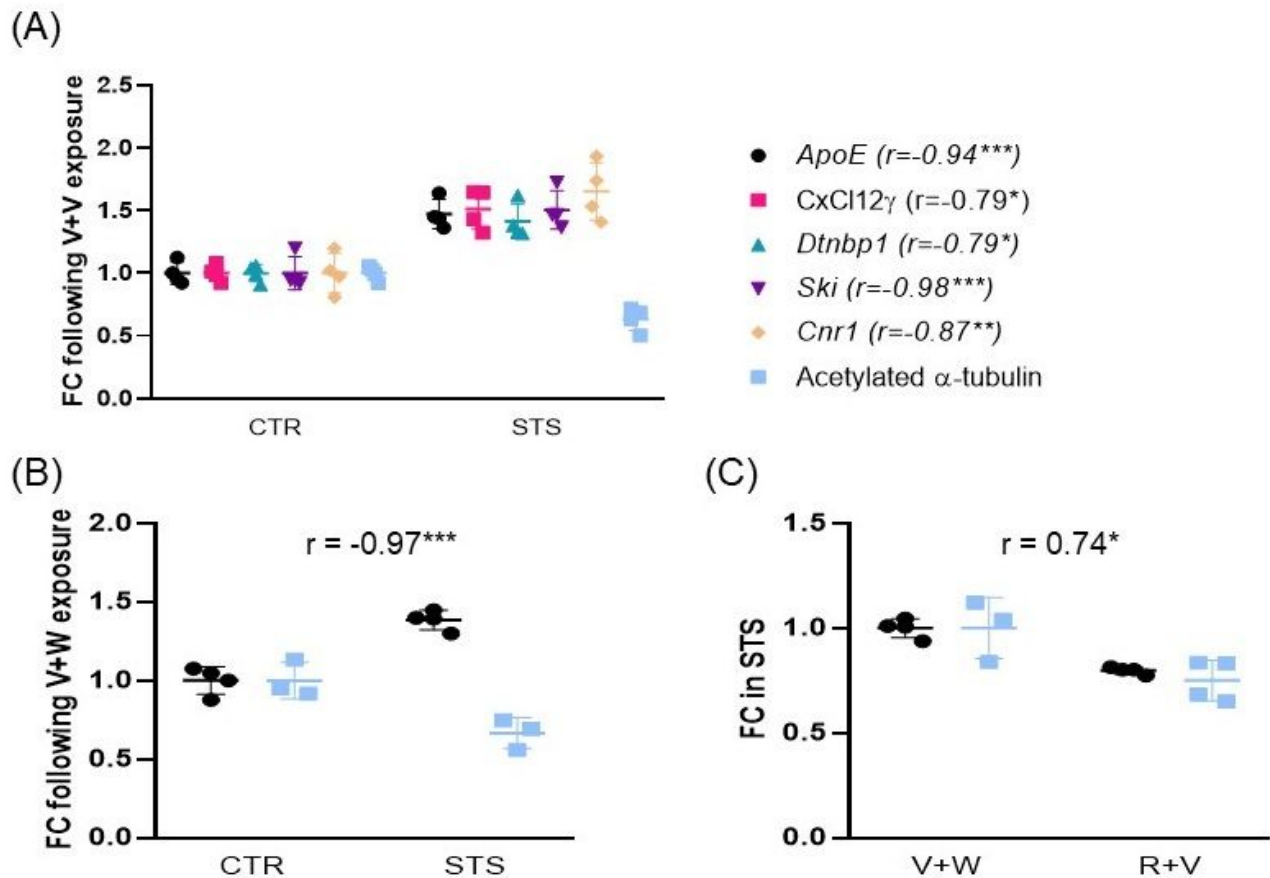


**Figure 4**

Correlation analysis between acetylated  $\alpha$ -tubulin at K40 and gene expression in the prefrontal cortex. We reported an inverse association between acetylated  $\alpha$ -tubulin levels and either ApoE, CxCl12 $\gamma$ , Dtnbp1, Ski, or Cnr1 when compared controls and defeat mice subjected to V+V (panel A); and also did the expression of ApoE upon V+W treatment when comparing the control and the stress group (panel B). A positive correlation between acetylated  $\alpha$ -tubulin and ApoE was reported between V+W and R+V under stress conditions (panel C). CTR, control; STS, stress; V, vehicle; W, WIN55,212-2; R, rimonabant. One, two or three symbols indicate  $P < 0.05$ ;  $P < 0.01$ ,  $P < 0.001$ , respectively.

## Supplementary Files

This is a list of supplementary files associated with this preprint. Click to download.

- [FigS1.pptx](#)